

Paramagnetic Levitational Assembly of Hydrogels

SUPPORTING INFORMATION

DOI: 10.1002/ adma.201200285

Dr. S. Tasoglu Author-One, D. Kavaz Author-Two, Dr. U. A. Gurkan Author-Three, Dr. S. Guven Author-Four, Dr. P. Chen Author-Five, R. Zheng Author-Six, Dr. U. Demirci Corresponding Author,

Bio-Acoustic MEMS in Medicine (BAMM) Laboratory, Division of Bioengineering,
Department of Medicine, Brigham and Women's Hospital, Harvard Medical School, Boston,
Massachusetts 02115, USA

Harvard-MIT Health Sciences and Technology, Cambridge, MA, 02139, USA

E-mail: udemirci@rics.bwh.harvard.edu

Surface field strength of magnets

The strength of the magnetic field at the surface of the magnets (diameter x length: 1/2" x 1", 5/16" x 1", 3/16" x 1"; KJ magnetics, CA) was measured using a handheld DC magnetometer (AlphaLab Inc, www.trifield.com) and given in Table S1.

Table S1: The strength of the magnetic field at the surface of the magnets (n =10).

		North Surface Magnetic Flux Density (Gauss)		South Surface Magnetic Flux Density (Gauss)	
diameter	height	Mean	Standard Deviation	Mean	Standard Deviation
1/2"	1"	5138.33	±0.94%	5145.67	±1.41%
5/16"		4688.17	±0.88%	4793.17	±0.85%
3/16"		4222.51	±1.03%	4312.14	±0.99%

Surrounding liquid effects on hydrogel motion in magnetic field

We have initially explored the potential for pseudo-forces as well as potential exclusion of hydrogels due to a diamagnetic effect of water for the hydrogel movement in a magnetic field. However, we observed motion of hydrogels towards the magnet for all experiments. The motion of a single hydrogel under a magnetic field can't be explained by the pseudo-forces, as hydrogels are obviously tracking the magnet (please see Movie S1). In all of the videos, we observed that hydrogels were pulled by the permanent magnet and there was an active attraction. In the video, a permanent magnet was fixed (not moving) above the fluid reservoir, and a single hydrogel was placed onto a far location from the magnet. If the driving force was the diamagnetic water motion from higher magnetic field to lower magnetic field, such phenomenon would create a source-like motion in physics, *i.e.* constant radial movement of water molecules from the centroid of magnet towards outward. Such motion would always move hydrogels outward from magnet centroid where it will be the "source" location. Contrarily, we observed that hydrogels moved toward the magnet centroid.

Assumptions of the computational model

During the experiments, hydrogels were placed at the surface of fluidic reservoir just below the air interface. Since the magnetic susceptibilities of the air above the liquid reservoir and the liquid (PBS) inside the reservoir are very close to 1, the Maxwell equations were solved assuming that the entire surrounding medium has a single susceptibility value. 1 mm x 1 mm x 150 μ m hydrogels were used, as it was easier to track them in the video analysis, to compare experimental results and model simulations. The assumptions of the computational and mathematical model are given in detail in Table S2.

Table S2: Assumptions in the computational and mathematical model

Surrounding medium is assumed to have a spherical shape. Center of sphere (surrounding medium) and center of cylindrical magnet are set to the same location. This assumption allows vanishing boundary affects, which is valid for the experimental conditions considering the length scales of hydrogel and petri-dish.
Uniform susceptibility of polymer throughout the hydrogel volume
Stokes' drag force is valid for spherical objects. We chose a characteristic length of hydrogel, and used it as length scale in Stokes' drag equation.
Best curve-fit into the magnetic forces calculated by the computational model is Gaussian 6 th order fit.
We assume that there are two active forces: (i) magnetic forces (calculated by the computational model, as a function of location of hydrogel) and (ii) drag forces exerted by the liquid environment. Gaussian 6 th order fit is included into the analytical model.

Additional computational model results

Decreasing the gap between the magnet and the hydrogel enhanced magnetic force amplitude on the hydrogel (Figure S1A and S1B).

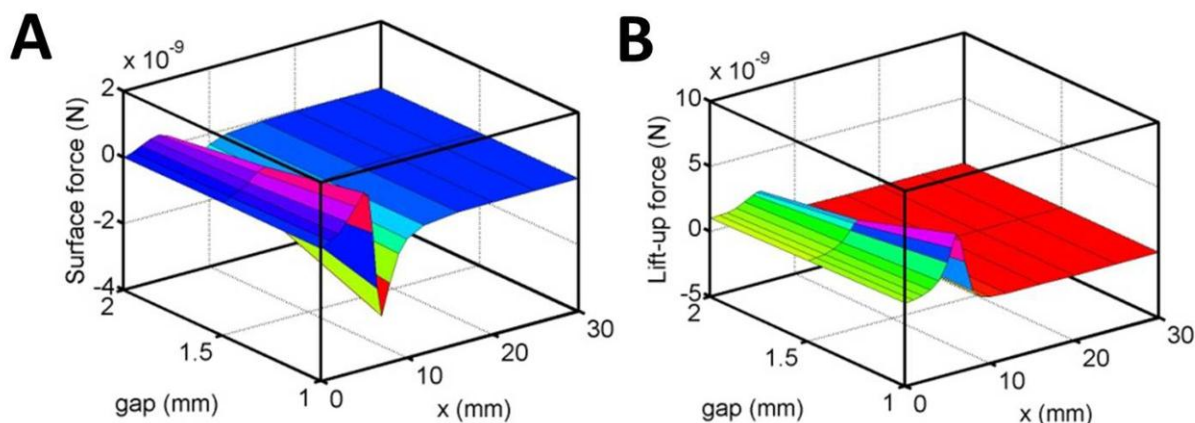


Figure S1. (A) Surface (along the direction of motion) and (B) Levitational (normal to direction of motion) magnetic forces as a function of the gap size and horizontal “x” location.

We have fabricated a simple setup to record the motion of a hydrogel (Figure S2). To get the images of the gel under a magnet, we fixed the camera at an angle of 30° to the horizontal. Note that, this angle does not affect the results as long as the area under magnet is seen by the camera. Two lines, perpendicular to each other were printed on the paper and considered as the X (along the direction of motion) and Y axes (vertical to the direction of motion). This coordinate paper was placed under the petri-dish to get the accurate location and also to track the trajectory of the gels. In all experiments, a gel was first placed at ($x = 2.5$ cm, $y = 0$ cm) and movement to the magnet was recorded along the parallel line to reduce the error of the gel location. The center of the magnet is fixed at $x = 0$ cm.

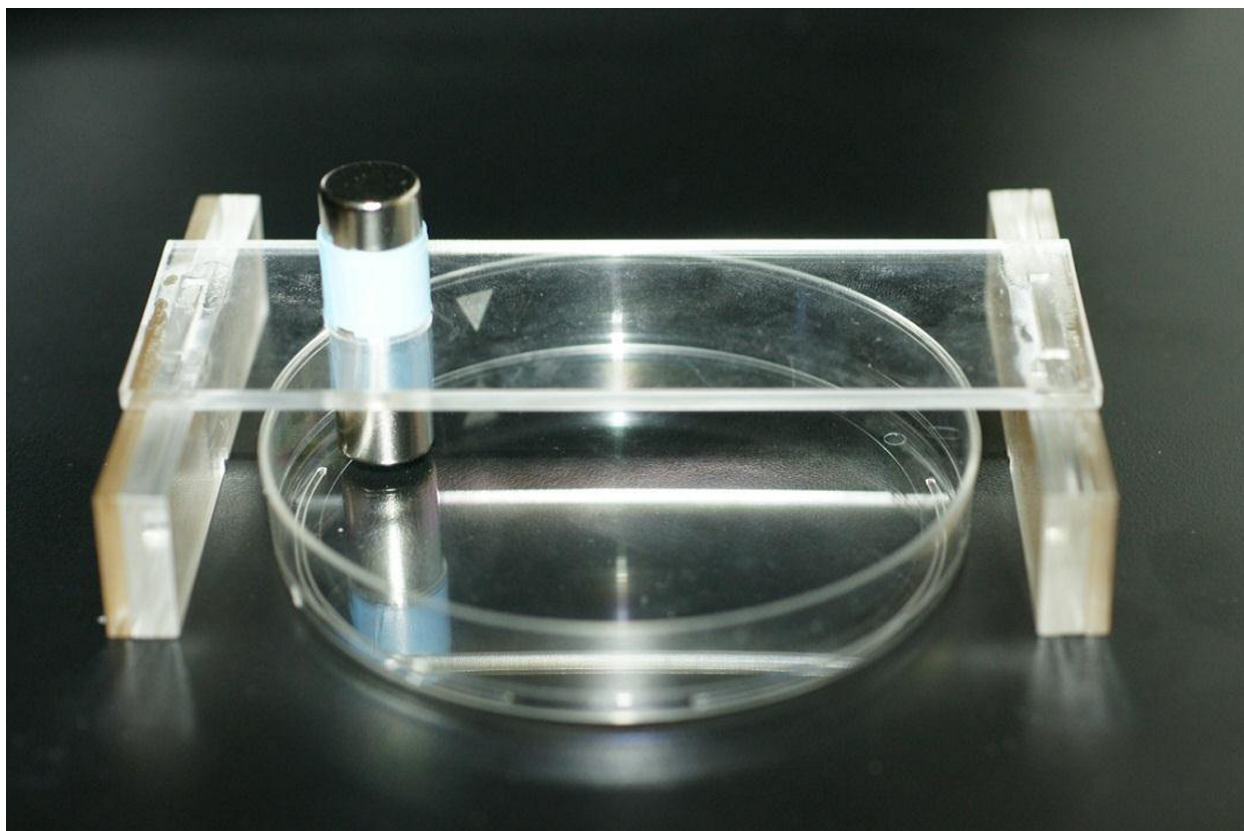
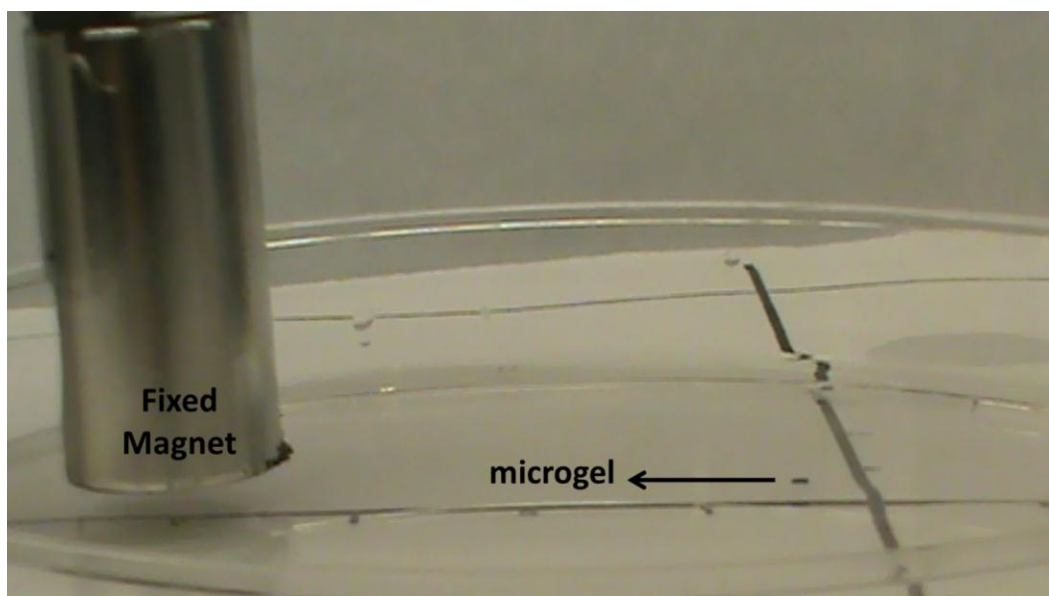


Figure S2. The platform to measure the hydrogel velocity under a magnet. The diameter of the cylindrical magnet is 1/2 inches



Movie S1. Still image of the video of hydrogel motion. The diameter of the cylindrical magnet is 1/2 inches

Paramagnetic response of PEG hydrogels

We performed following spectroscopic and chemical experiments as a function of UV exposure time to investigate the origins of magnetic response of PEG hydrogels:

- Raman spectroscopy measurements to show the crosslinking of PEG hydrogels
- Velocity analyses for three control groups:
 1. Control A: irradiate a PEG hydrogel considerably more than in our standard samples for multiple irradiation times,
 2. Control B: crosslink a PEG hydrogel using a chemical method without UV exposure,
 3. Control C: irradiate a chemically synthesized PEG hydrogel with UV.
- Electron paramagnetic resonance (EPR) spectroscopy measurements to quantify free radical formation

Raman Spectroscopy

We have performed Raman spectroscopy to validate the photo-crosslinking of hydrogels. Uncrosslinked sample containing PEGDMA and photo-initiator, PI, (Igracure 2959, Ciba) (Fig. S3A) shows typical characteristic peaks for PEG and methyl acrylate group (Fig. S3B). Characteristic bands for PEG are C-O-C peaks appearing at 851.3 cm^{-1} , 1042.6 cm^{-1} and 1138.7 cm^{-1} . Methyl acrylate group can be distinguished from C=O (1700 cm^{-1}) peak and C=C (1637 cm^{-1}) peak which disappear upon photo-crosslinking. Presence of PI in uncrosslinked sample can be easily detected from aromatic ring peak (1598.7 cm^{-1}) [1]. Photo-crosslinking of PEGDMA is propagated by radical formed after UV irradiation of the PI. Formed radical attacks acrylate C=C bond resulting in formation of secondary alkyl radical (CH \cdot) and formation of C – C bond. Crosslinking reaction continues through the secondary alkyl radicals that attacks to another C=C bond in another PEGDMA chain. This chain reaction eliminates C=C bonds present in the system and crosslinks PEGDMA chains. With our system and setup we show reduction of C=C peak (1637 cm^{-1}) with UV exposure in PEG hydrogels. The intensity of -C-O-C- and -CH $_2$ peaks indicates the degree of photo-crosslinking depending on different UV exposure times (Fig. S3B). The estimated resulting cross-linked PEGDMA network is shown in Fig. S3A.

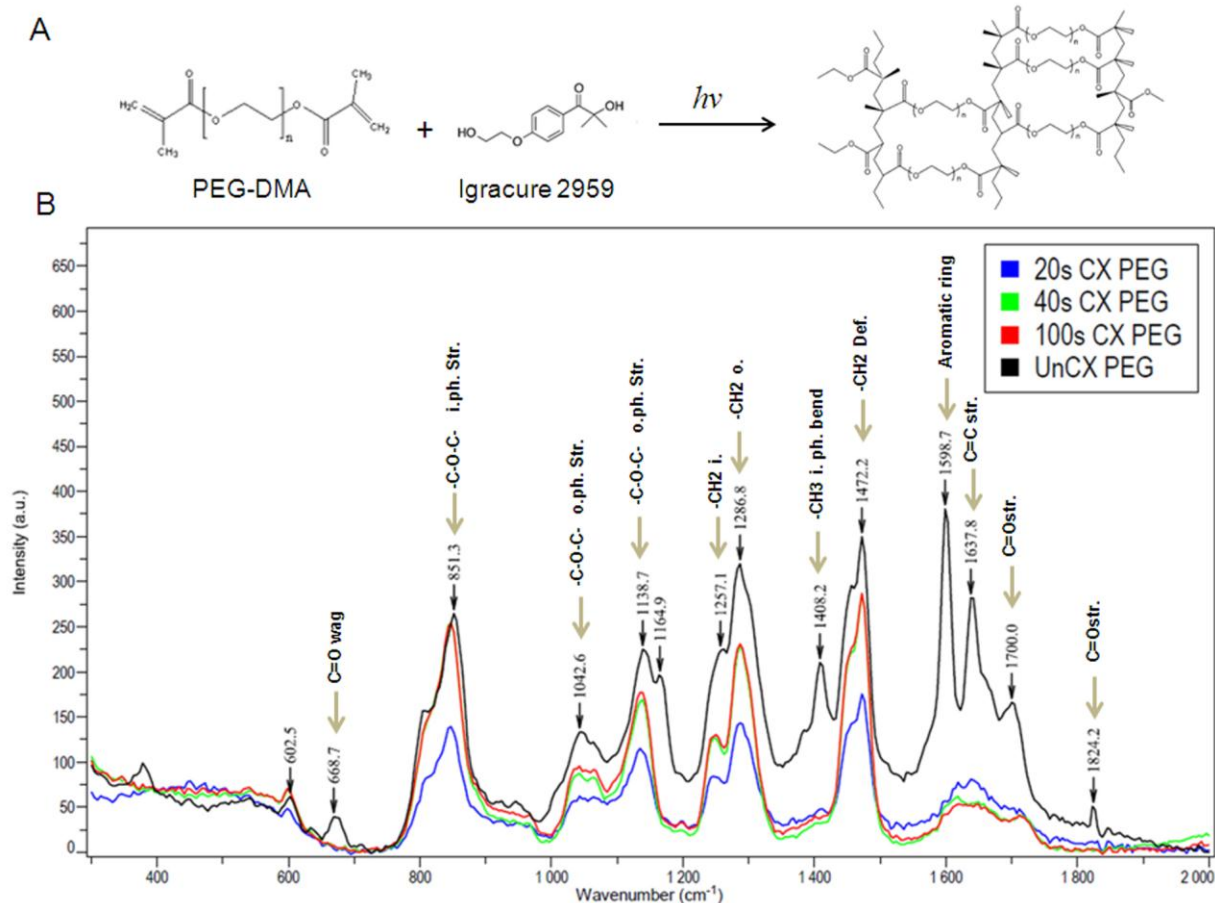


Figure S3. A) Schematic representation of photo-crosslinking of PEGDMA with Irgacure 2959, and formed network, B) Raman spectroscopy of uncrosslinked and different UV exposure time polymerized PEG hydrogels. Crosslinking is achieved through C=C (1637 cm^{-1}) by secondary alkyl radical formation.

Velocity analyses for three control groups

To evaluate magnetic response of hydrogels, we first fabricated photo-cross-linked gels with various UV exposure times (20 sec, 40 sec, and 100 sec). Second, we utilized chemically cross-linked PEG gels with and without UV exposure. We evaluated the free radical formation in these gels by EPR and how the gels respond to magnetic field.

Control A: We first fabricated UV cross-linked hydrogels for a range of UV exposure time of 20 sec, 40 sec, and 100 sec, and recorded the gel motion under a magnet using the setup shown at the inset of Fig. S4. Results showed that the hydrogels that were exposed to UV for longer durations travelled towards the magnets with a higher velocity (please see Movie S2-4). These results clearly support the correlation between irradiation time and magnetic response of hydrogels. As shown in the next section, EPR analysis indicated the existence of more free radicals as UV exposure time was increased (Fig. S5).

Gel Velocity vs Position for a range of crosslinking time

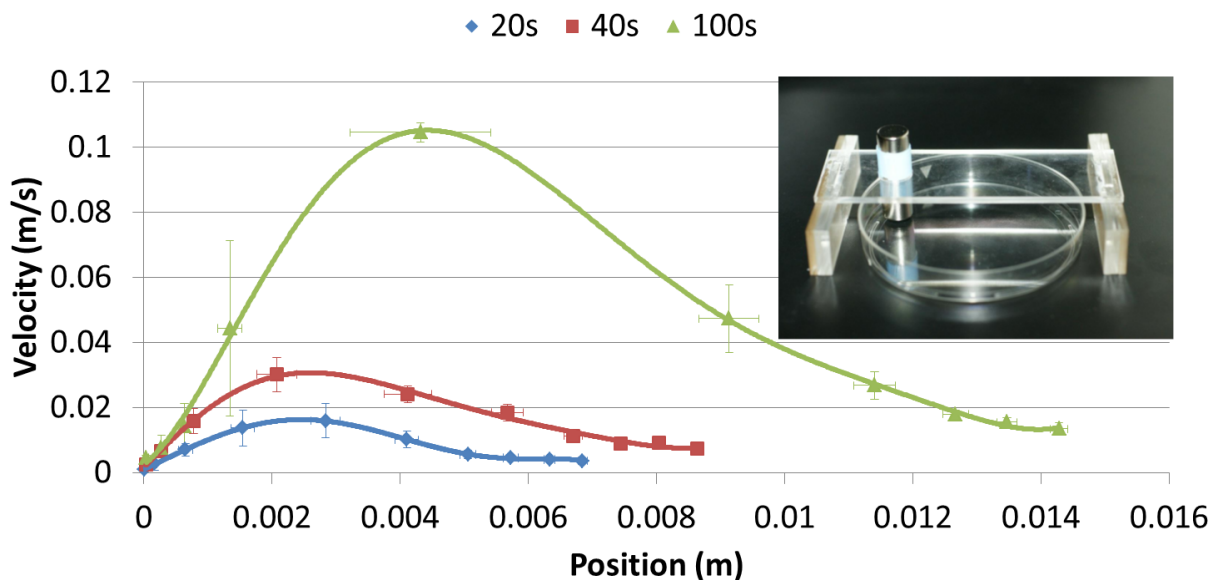


Figure S4. Gel velocity vs. gel location for a range of UV exposure time (20 sec, 40 sec, and 100 sec). A cylindrical NdFeB magnet is fixed above a petri-dish filled with PBS ($x = 0$ at centroid of the magnet). PEG hydrogels move faster towards the magnet, as the UV exposure time increases.

Control B: We have fabricated chemically cross-linked hydrogels (see experimental methods) using the same polymer (*i.e.*, PEGDMA) and ammonium persulphate (APS) as the chemical crosslinker [2]. We performed the same velocity experiment, and placed a chemically cross-linked hydrogel into the velocity setup (inset of Fig. S4) without UV exposure. We observed that PEG hydrogels fabricated for a range of APS concentration (from 1 to 10% w/w), did not respond to magnetic field (please see Movie S5). As shown in the next section, EPR analysis indicated that there were not any detectable remaining free radicals in the chemically cross-linked hydrogel (Fig. S6).

Control C: We irradiated chemically synthesized hydrogels (same hydrogels as Control B) with UV. For each APS concentration (1, 5, and 10% w/w), UV was applied up to 400 sec on these gels. We expect that Control C has been already chemically cross-linked, therefore all the carbon double bonds $C=C$ have been already saturated. In this experiment, we did not observe response from Control C to magnetic field. These findings are in parallel with the EPR results for Controls B and C showing that there are not any detectable remaining free radicals in these gels as discussed in the next section.

Electron paramagnetic resonance (EPR) measurement

We performed electron paramagnetic resonance (EPR) measurements to evaluate free radical formation in PEG hydrogels prepared by both photo-crosslinking and chemical crosslinking.

EPR spectra of UV cross-linked PEG hydrogels (PEGDMA 1000 with 1% photo-initiator) were given in Fig. S5. PEG hydrogel precursor solution without UV exposure was used as a control

group. The result showed that PEG hydrogel precursor solution without UV exposure gave no EPR signals. After 20 sec and 100 sec UV photo-crosslinking, PEG hydrogels had strong signals between 3450 G and 3600 G, which indicated the formation of free radicals in the hydrogels (Control A). Resulting spectrum shows 5 peaks corresponding to expected secondary alkyl radical formed after UV exposure [3, 4]. Furthermore, 100 sec UV photo-crosslinking gave higher signals compared to 20 sec UV exposure, which indicated that the amount of free radicals was correlated with exposure time (Control A). Although EPR measurements showed that free radical formation increased with UV exposure time, further investigation needs to be performed to ensure that magnetic response of hydrogels is due to the free radical formation.

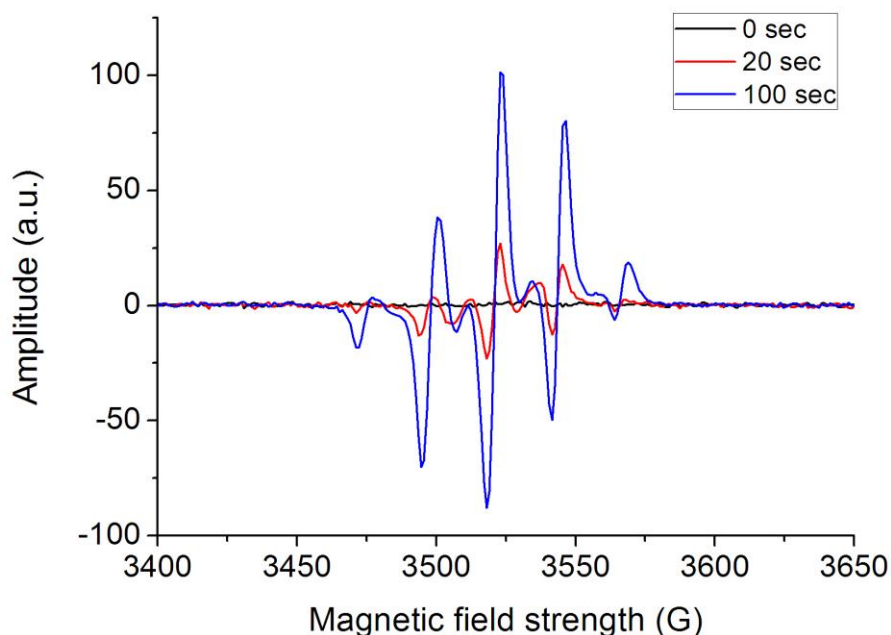


Figure S5. EPR spectra of photo-cross-linked PEG 1000 hydrogels with 20 sec and 100 sec exposure time. PEG hydrogel precursor solution (PEGDMA 1000 with 1% photo-initiator) without UV exposure was used as a control group. Analysis has been performed with the sum of 10 scans for each condition.

EPR spectra of chemically cross-linked PEG hydrogels (Control B & C) were shown in Fig. S6. No signal was found in chemically cross-linked PEG hydrogels without any UV exposure (Control B) or with UV exposure (Control C). In this condition ammonium persulphate was used as an initiator of crosslinking reaction where remaining free radicals were not detected by the EPR system. These results are in parallel with the observation that Control B & C did not respond to magnetic field that we observed in the velocity experiments (Fig. S4).

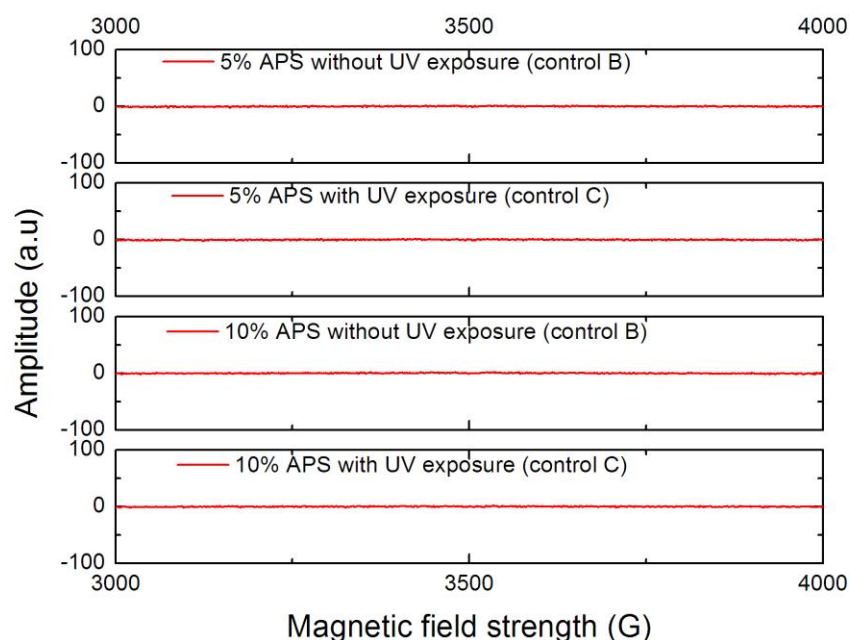


Figure S6. EPR spectra of chemically cross-linked PEG 1000 hydrogels. PEGDMA 1000 was liquidified at 37°C and mixed with 5 and 10% w/w ammonium persulphate (APS) (Sigma). First and third rows are chemically synthesized gels without UV exposure (Control B), second and fourth rows are UV irradiated chemically synthesized gels (Control C). Analysis has been performed with the sum of 10 scans for each condition.

Proliferation capacity of PEG hydrogels

PEG gels are reported earlier to have proliferation capacity for high molecular weight [5]. To show proliferation capacity of encapsulated cells, we have performed immunocytochemistry (ICC) on hydrogels on day 10. PEG hydrogels were stained with specific nuclear proliferation marker Ki67 (Abcam, MA, USA). Staining is explained in detail in section *Ki67 Staining for PEGDA 4000 UV cross-linked gels*. All experimental conditions were Ki67 positive indicating that encapsulated cells were proliferating after 10 days of encapsulation. Ki67 is a nuclear marker and co-localizes within the nuclei with DAPI staining. Low magnification images show that majority of cells were proliferating and evenly distributed within hydrogels (Fig 5H-J).

We have also performed Alamar Blue, cell viability assay at day 7 on photo-cross-linked hydrogels with various UV exposure times to support our Live/Dead assay presented in the manuscript. Details are given in section *Cell viability and proliferation*. Alamar Blue assay is based on metabolic activity of encapsulated cells. Higher fluorescence intensity indicates higher number of viable cells.

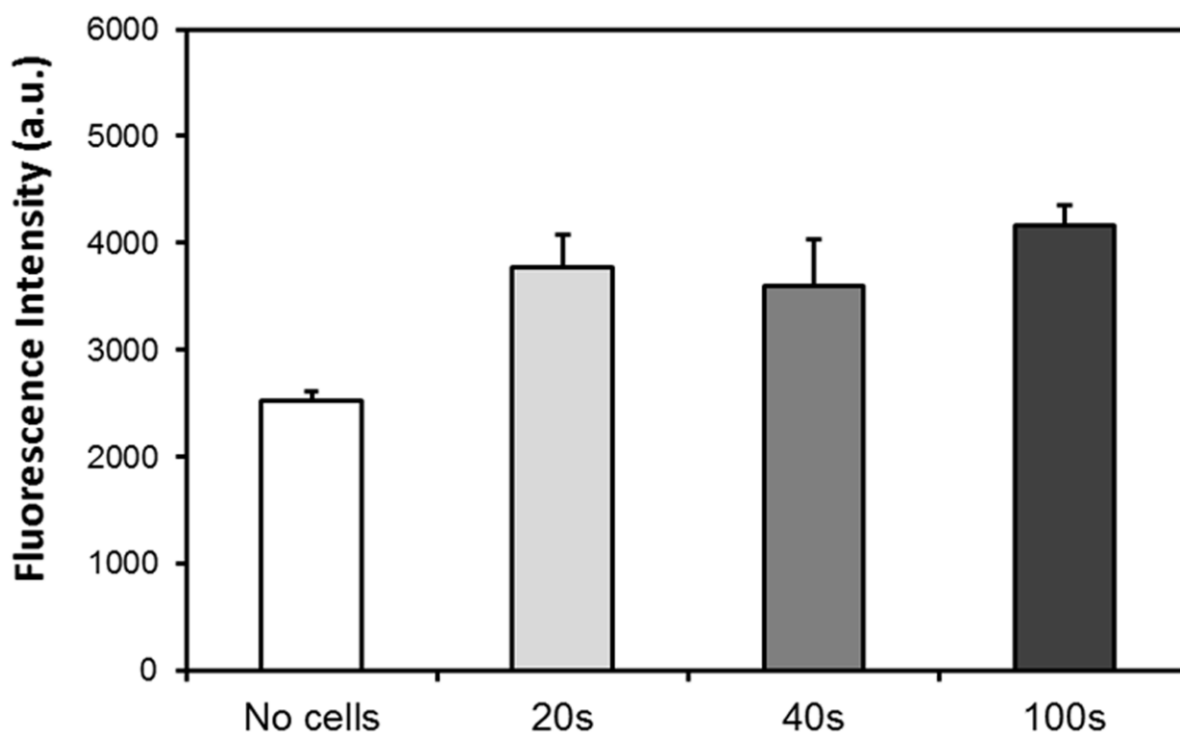


Figure S7. Alamar blue cell viability assay has been performed after 7 days of cell encapsulation. Viability of 3T3 cells in different photo-crosslinking times show similar trend and significant difference compared to gels with no cells as controls (n=12-15, p<0.05, ANOVA).

Experimental Methods

Fabrication of Microgels

Microgels were fabricated by dissolving (20%, wt/wt) Poly(ethylene glycol) dimethacrylate (PEGDMA; MW 1000; Polysciences) in Dulbecco's phosphate-buffered saline (DPBS, GIBCO). Then, 2-hydroxy-1-(4-(hydroxyethoxy)phenyl)-2-methyl-1-propanone photoinitiator (1%, wt/wt, Irgacure 2959; CIBA Chemicals) was added to the prepolymer solution. In this study, we used four types of photomasks with square patterns and of different sizes (200 x 200 μm^2 , 400 x 400 μm^2 , 500 x 500 μm^2 , and 1000 x 1000 μm^2) (Figure 1A). A 20 μl droplet of photocrosslinkable PEG prepolymer solution was pipetted onto a glass slide covered by a cover slip and separated by spacers (cover slip 25 x 25 mm^2 , thickness: 150 μm). The photomasks were placed on the cover slip between the UV light and prepolymer. Another 25 x 25 mm^2 coverslide was placed onto the droplet. Microgels were fabricated by exposing the gel prepolymer solution to UV light (500 mW; at a height of 50 mm above the microgels) for 20 seconds, for polymerization to take place on the surface of the glass slide. Then, the photomask and glass cover slip were removed and microgels were obtained. Using a scalpel, the microgels were removed and left to soak in DPBS solution in a standard 60 x 15 mm^2 Pyrex reusable Petri dish (Fisher Scientific).

Experimental Setup

The fabricated microgels were suspended in DPBS solution in petri dishes. We observed that a fraction of the fabricated microgels were most responsive to the magnetic field at every batch. We worked with these responsive microgels in the experiments. They were assembled in various shapes with the help of manually controlled cylindrical magnets (1 mm above the gels, Figure 1). Microgels were directed towards a prespecified location one-by-one using the magnetic field and assembled there to form geometrical shapes. Various magnet sizes (diameter x length: 1.2 x 2.4 cm, 0.8 x 2.4 cm, 0.5 x 2.4 cm; KJ magnetics, CA) were used, and the number of assembled gels for each magnet size were evaluated.

Secondary Cross-Linking to Stabilize the Microgel Assembly

The microgels were assembled on the surface of the DPBS solution and 500 μ L prepolymer solution was added to assembly. The microgels were exposed to secondary UV cross-linking for 20 seconds to stabilize the shape of the structure. To visually differentiate microgels, we used fluorescent dye, fluorescein isothiocyanate-dextran (FITC-dextran, $M_r = 2,000$ kDa), Rhodamine-B ($M_r = 10$ kDa), and food dye. Dyes were mixed with prepolymer solution at a concentration of 0.2 mM before photocrosslinking.

Assembly and Patterning of Microgels in a Chamber

To establish an assembly system, where multiple groups of gels were kept in reservoirs, we constructed a chamber by sandwiching alternating layers of 3 mm thick poly (methylmetacrylate) (PMMA) and 50 μ m thick double-sided adhesive (DSA) between adjacent plates of PMMA (8.5 cm x 12 cm). The chamber was built with five layers of plastic and four layers of adhesive film. The device was composed of three circular peripheral wells all connecting to primary rectangular well. At the bottom, there was one layer of PMMA without wells. The other four layers of PMMA and DSA consist of wells. The whole chamber was specially designed as a celtic-shaped chamber, which was used to pattern gels in different orientations (Figure 3E). All wells were cut using a laser cutter (VersaLaser™, Scottsdale AZ). Microgels suspended in PBS (5 mL) were pipetted into the chamber. Neodymium magnets (1.2 x 2.4 cm, K&J Magnetics, CA) were placed over the gels. With the help of these magnets, selected colored gels were moved through the rectangular part of the chamber one-by-one to create different shapes of assembled microgels. Each microgel is moved from chambers by applying magnetic field on it. We directed microgels one-by-one from chambers to the thin channel of the celtic chamber to assemble the gels. After a microgel is parked into the thin channel, it is exposed to decelerating forces as both walls are close to parked microgel. Therefore, previously parked microgels were immobilized easily while second or third microgel was moved next to the parked microgel(s).

Layer by Layer Assembly of Microgels

To assemble multiple layers of microgels, the first layer of microgels were assembled into a square shaped structure. After a single layer was assembled, the construct was stabilized by adding PEG prepolymer solution (20 μ L) followed by a second UV crosslinking. Then, the assembly process was repeated to build a second layer on top of the first. The two-layer construct was stabilized by adding PEG solution (20 μ l) followed by a second UV crosslinking. Figure 3C showed that the merged image of a square shaped 3D assembly. The first layer of gels were stained with Rhodamine-B, the second layer of gels were stained with FITC-dextran, the third layer of gels were stained with Rhodamine-B again. The images were merged showing all three layers.

Quantification of Assembled Microgels

We also analyzed resulting types of microgel assemblies. Gels were assembled to form different shapes, and classified according to the number of observed shapes during the experiments (Figure 4). Each shape was imaged by using a digital camera (Canon A3300IS).

Quantification of Microgel Number by Using Different Size Magnets

We manually recorded the number of microgels assembled under different size of magnets and for a range of microgel size (Figure 4F). Data collected in this study were reported as mean \pm standard error of the mean. The results were assessed using analysis of variance (ANOVA) with Tukey's post-hoc comparison. Statistical significance was set at 95% confidence level for all tests ($p < 0.05$). The experiments were repeated at least four times to validate repeatability and reproducibility. Error bars in the figures represent standard error of the mean.

Cell Encapsulation

NIH 3T3 fibroblasts were used in this study. The cells were cultured in Dulbecco's modified Eagle's medium (DMEM; Sigma-Aldrich) supplemented with 10% fetal bovine serum (FBS; GIBCO) in a 5% CO₂ humidified incubator at 37 °C. To harvest and encapsulate cells, the cells were first trypsinized with 1% trypsin (GIBCO) and centrifuged at 1000 rpm for 5 min. At a density of 1×10^7 /mL, the cells were suspended in the PEG prepolymer solution. Cell encapsulating microgels were then fabricated (Figure 1B). The cell encapsulating microgels were first washed with DPBS and then, incubated with live/dead dyes for 15 min. The live/dead dyes were prepared by diluting 2 ml of Calcein AM, and 0.5 ml of Ethidium homodimer-1; Molecular Probes in 1 ml of DPBS. Cells were labeled green with Calcein AM and labeled red with PKH26 Red Fluorescent cell linker. After encapsulation, cell viability was examined using a live/dead assay (Molecular Probes, Invitrogen). The fluorescent images were taken using an inverted fluorescent microscope (Nikon, TE2000). All the images were taken after 1 day, 3 days, 5 days and 7 days of culture. The controls were cells in culture without gels (Figure 5). Cell viability was also quantified by using AlamarBlue (Invitrogen) reagent. Cell encapsulating microgels were first washed with DPBS and AlamarBlue reagent was added into each flask, followed by 4 hours of incubation at 37°C. The AlamarBlue reagent was prepared by diluting 1 mL of dye in 10 mL DMEM. There was no immediate color change in any flasks upon addition. After 4 hours, all flask were then rechecked for color change. The resulting fluorescence was read on a plate reader. The absorbance of AlamarBlue reagent was read on a spectrophotometer (wavelength = 570-600 nm). Finally, results were compared by plotting cell viability percentage after each step.

Staining hydrogels

The dye is composed of small molecules and has a minor interaction with the polymer. The dye demonstrated enough interaction to stay for sufficiently long time in the hydrogel for the assembly process and can be seen during the video recording. Gels with and without the fluorescent dye moved with similar kinematic characteristics.

Image Recording and Processing

The images were captured by a digital camera (Canon A3300IS) and, videos were recorded by a camcorder (Sony Handycam HDR-CX160). To enhance the visibility of the hydrogels in PBS,

blue food dye was added to the prepolymer solution. For validation of the hydrogel motion, kinematic data was extracted from recorded video of hydrogel motion (supplementary video) (ImageJ, MTrackJ plugin). Cell viability was quantified by analyzing the images using public domain NIH ImageJ program (developed at the U.S. National Institutes of Health and available at <http://rsb.info.nih.gov/nih/image/>). Characterization was done at three time points, *i.e.*, 6h after preparation of cell-encapsulated hydrogels, and 1 day and 3 days after culture.

Raman analysis

The PEG hydrogels were prepared at varying crosslinking durations (20 sec, 40 sec, and 100 sec) for Raman Analysis. Raman spectra were obtained using 532 nm laser and a confocal Raman Microscope (WITec CRM-200, WITec Instruments Corp., Knoxville, TN). Raman system was first calibrated using a standard Si sample. Uncrosslinked PEG was used as a control sample. A wavenumber range of 300-2000 cm^{-1} was selected to visualize the characteristic peaks of PEG hydrogel. Raman spectra were collected from at least 2 samples per group.

Preparation of chemically cross-linked PEG gels

20% w/v PEGDMA 1000 (Polysciences) was dissolved in PBS (Gibco, Invitrogen) and mixed with 1 to 10% w/v ammonium persulphate (APS) (Sigma). Prepared polymer solution was pipetted into 150 μm deep and 1mm x 1mm sized wells made of PDMS. Crosslinking was achieved by incubating loaded PDMS mold at 37°C for 2 h to 2 days (depending on the APS concentration).

Sample preparation for Electron Paramagnetic Resonance (EPR) measurements

For fabrication of UV cross-linked PEG hydrogels, poly(ethylene glycol) (1000) dimethacrylate (PEGDMA, Polysciences, Inc.) was melted in the water-bath with 1-10% (v/v) photo-initiator (2-Hydroxy-4'-(2-hydroxyethoxy)-2-methylpropiophenone, irgacure 2959, Sigma). 5 μL PEG prepolymer was loaded into EPR tubes and then exposed to UV light for 20 sec and 100 sec respectively. Chemically cross-linked hydrogels were fabricated as described in *Preparation of chemically cross-linked PEG gels* section.

Electron Paramagnetic Resonance (EPR) spectrum measurement

EPR was carried out using a Bruker EMX EPR Spectrometer, an ER 4199HS cavity and a Gunn diode microwave source (8-10 GHz, X-band). Parameters used in the experiments are as follows: microwave frequency, 9.871 GHz; microwave power: 0.638 mW; receiver modulation frequency: 100.00 kHz; modulation amplitude: 1.00 G; signal channel time constant: 20.480 msec. UV cross-linked and chemically cross-linked PEG hydrogels were measured by the EPR immediately after fabrication separately.

SU-8 mold fabrication

4-inch silicon wafer (University Wafer, MA) was used as a substrate material and cleaned by solvents (acetone, isopropanol), dehydrated at 200°C for 5 min on a hot plate and cooled with nitrogen. Subsequently, oxygen plasma cleaning was performed using Plasma Stripper (oxygen flow rate: 20 sccm; chamber pressure: 300 mTorr; and power: 150 W) for 3 min. A thin layer of OmniCoat™ (MicroChem) was first coated on the wafer surface (3000 rpm for 30 sec) to enhance adhesion between silicon wafer and the photoresist, followed by curing at 200°C for 1 min. SU-8 2100 photoresist (MicroChem) was poured on the center of the wafer and spun at 1900 rpm for 45 sec, followed by soft baking (65°C for 5 min and 95°C for 30 min on a hot

plate) and edge bead removal. Subsequently, UV exposure was conducted with the exposure energy of 260 mJ/cm^2 by SUSS MJB4, followed by post expose bake (65°C for 5 min and 95°C for 12 min on a hot plate) and development using SU-8 developer (MicroChem) for 17 min. Finally, hard bake (150°C for 20 min) was used to cure final mold (Fig. S8). Before using, SU-8 mold was coated by Trichloro(1H,1H,2H,2H-perfluorooctyl)silane (Sigma) to allow easy release of the PDMS structure.

PDMS mold fabrication

Polydimethylsiloxane (PDMS) prepolymer was prepared by mixing PDMS-Sylgard Silicone Elastomer 184 and Sylgard Curing Agent 184 (Dow Corning Corp) with a ratio of 10:1. After degassing, the prepolymer was poured on the SU-8 mold in a Petri dish, followed by the second degassing and curing at 80°C for 3 h in the oven. Subsequently, PDMS layer was cut and peeled off from the SU-8 mold (Fig. S8).

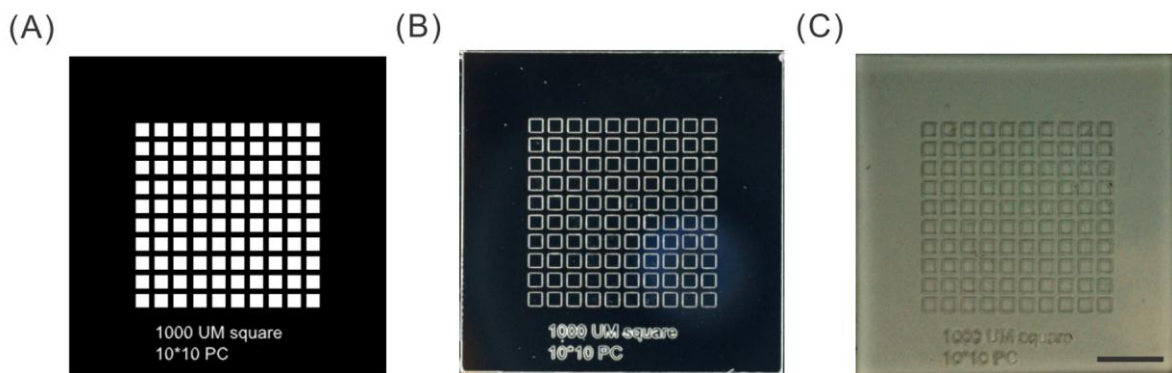


Figure S8. Mold fabrication for chemical cross-linking hydrogels. (A) Photomask for photolithography, (B) SU-8 positive mold on silicon wafer substrate, (C) PDMS negative mold. Scale bar indicates 5 mm.

Cell viability and proliferation

3T3 fibroblast cell line with 10^7 cell/ml density were encapsulated in 20% w/v PEG 4000 (Polysciences) dissolved in PBS (Gibco, Invitrogen), mixed with 1% w/v of photo-initiator (Irgacure, Ciba). Photo-crosslinking was performed with 500 mW UV light for 20, 40 and 100 sec. Prepared hydrogels were incubated in agarose coated cell culture plates for 7 days. To access viability and metabolic activity an alamar blue staining has been performed at day 7 following encapsulation. Briefly, alamar blue (Invitrogen) has been added to each crosslinking condition with 1:10 volume ratio to the cell culture media and incubated for 3h at 37°C , 5% CO_2 humidified incubator. Following the incubation fluorescence was measured at ex560nm / em590nm plate reader. Cell free gels were used as controls. Decreasing fluorescence intensity refers to lower metabolic activity within PEG hydrogels.

Ki67 Staining for PEGDA 4000 UV cross-linked gels

3T3 cells encapsulating gels were fixed with 1% paraformaldehyde for 1h at room temperature (RT) and washed. Gels were permeabilized with 0.3% Triton-X 100 (Sigma), in 1% BSA (Sigma), for min 1h at RT. Gels were stained with Rb mKi67 (Ab16667, Abcam) overnight at 4°C . After washing, gels were incubated with secondary antibody goat anti rabbit Alexa Fluor

564 (A11011, Invitrogen) for 2h at RT. DAPI was used as nuclear counter staining. After washing hydrogels were visualized under fluorescent microscope (Zeiss AXIO).

Statistical Method

Fluorescent intensity measurements obtained from Alamar blue cell viability assay (n=12-15) were statistically compared using parametric one way analysis of variance (ANOVA) with Tukey's posthoc test for multiple comparisons. Statistical significance threshold was set at 0.05 (p<0.05).

References:

1. Larkin, P.J., *IR and Raman Spectroscopy Principles and Spectral Interpretation*. 2011, Waltham, MA, USA: Elsevier.
2. Betz, M.W., et al., *Cyclic acetal hydrogel system for bone marrow stromal cell encapsulation and osteodifferentiation*. *Journal of Biomedical Materials Research Part A*, 2008. **86A**(3): p. 662-670.
3. Mellott, M.B., K. Searcy, and M.V. Pishko, *Release of protein from highly cross-linked hydrogels of poly(ethylene glycol) diacrylate fabricated by UV polymerization*. *Biomaterials*, 2001. **22**(9): p. 929-941.
4. Lund, A., M. Shiotani, and S. Shimada, *Principles and Applications of ESR Spectroscopy*. 2011, Heidelberg: Springer.
5. Bharadwaj, S., et al., *Higher Molecular Weight Polyethylene Glycol Increases Cell Proliferation While Improving Barrier Function in an In Vitro Colon Cancer Model*. *Journal of Biomedicine and Biotechnology*, 2011. **2011**.